Apodized photonic crystal waveguide gratings

Nobuhiro Yokoi, Takeshi Fujisawa, Kunimasa Saitoh, and Masanori Koshiba

Division of Media and Network Technologies, Hokkaido University, Sapporo 060-0814, Japan
yokoi@icp.ist.hokudai.ac.jp

Abstract: Apodized photonic crystal (PC) waveguide gratings are proposed to suppress sidelobes which appear in reflection spectra of usual PC waveguide gratings. By using specific functions (Gauss and Gauss-cosine functions) for the longitudinal refractive index distribution, it is possible to suppress sidelobes in the reflection spectra of PC waveguide gratings efficiently. The apodization is realized by simply changing diameters of dielectric pillars adjacent to the PC waveguide core. It is shown that by using Gauss-cosine functions for the apodization, Bragg frequency of the waveguide grating becomes insensitive to the magnitude of perturbation leading to the possibility of designing waveguide gratings with arbitrarily Bragg frequency and bandwidth by modulating geometrical parameters only.

OCIS codes: (230.0230) Optical devices, (230.1480) Bragg reflectors, (999.9999) Photonic crystal

References and links

1. J. D. Joannopoulos, P. R. Villeneuve, and S. Fan, "Photonic crystals: putting a new twist of light," Nature **386**, 143-149 (1997).
2. M. Koshiba, "Wavelength division demultiplexing and multiplexing with photonic crystal waveguide couplers," J. Lightwave Technol. **19**, 1970-1975 (2001).
3. E. A. Camargo, H. M. H. Chong, and R. M. E. L. Rue, "2D photonic crystal thermo-optic switch based on AlGaAs/GaAs epitaxial structure," Opt. Express **12**, 588-592 (2004), http://www.opticsexpress.org/abstract.cfm?URI=OPEX-12-4-588.
4. M. Soljačić, M. Ibanescu, S. G. Johnson, Y. Fink, and J. D. Joannopoulos, "Optimal bistable switching in nonlinear photonic crystals," Phys. Rev. E **66**, 055601(R), (2002).
5. Y. Sugimoto, H. Nakamura, U. Tanaka, N. Ikeda, and K. Asakawa, "High-precision optical interference in Mach-Zehnder-type photonic crystal waveguide," Opt. Express **13**, 96-105 (2005), http://www.opticsexpress.org/abstract.cfm?URI=OPEX-13-1-96.
6. T. Fujisawa and M. Koshiba, "Finite-element mode-solver for nonlinear periodic optical waveguides and its application to photonic crystal circuits," J. Lightwave Technol. **23**, 382-387 (2005).
7. T. Fujisawa and M. Koshiba, "An analysis of photonic crystal waveguide gratings using coupled-mode theory and finite-element method," Appl. Opt. to be published.
8. T. Erdogan, "Fiber grating spectra," J. Lightwave Technol. **15**, 1277-1294 (1997).
9. M. Koshiba, Y. Tsuji, and M. Hikari, "Time-domain beam propagation method and its application to photonic crystal circuits," J. Lightwave Technol. **18**, 102-110 (2000).
10. T. Fujisawa and M. Koshiba, "Time-domain beam propagation method for nonlinear optical propagation analysis and its application to photonic crystal circuits," J. Lightwave Technol. **22**, 684-691 (2004).
11. M. Tokushima, H. Yamada, and Y. Arakawa, "1.5-μm-wavelength light guiding in waveguides in square-lattice-of-rod photonic crystal slab," Appl. Phys. Lett. **84**, 4298-4300 (2004).
12. S. Assefa, P. T. Rakich, P. Bienstman, S. G. Johnson, G. S. Petrich, J. D. Joannopoulos, L. A. Kolodziejski, E. P. Ippen, and H. I. Smith, "Guiding 1.5 μm light in photonic crystals based on dielectric rods," Appl. Phys. Lett. **85**, 6110-6112 (2004).
13. C.-C. Chen, C.-Y. Chen, W.-K. Wang, F.-H. Fluang, C.-K. Lin, W.-Y. Chiu, and Y.-J. Chan, "Photonic crystal directional couplers formed by InAlGaAs nano-rods," Opt. Express **13**, 38-43 (2005), http://www.opticsexpress.org/abstract.cfm?URI=OPEX-13-1-38.
14. M. Soljačić, S. G. Johnson, S. Fan, M. Ibanscu, E. Ippen, and J. D. Joannopoulos, "Photonic-crystal slow-light enhancement of nonlinear phase sensitivity," J. Opt. Soc. Am. B **19**, 2052-2059 (2002).

1. Introduction

Optical devices based on photonic crystals (PCs) have attracted considerable attention in recent years because of their unique features such as a photonic band gap (PBG) effect, high anisotropies, and so on. Because these features enable the size of PC devices to be in the order of wavelength scale, various kinds of PC devices such as optical directional couplers, microcavities, and Mach-Zehnder interferometers, have been studied so far [1]-[6]. More recently, waveguide gratings based on PCs were proposed as an alternative component for realizing ultrasmall optical functional devices [7]. Waveguide gratings play a very important role in integrated photonics, and can be used for various optical devices, for example, as wavelength filters, mode converters, reflectors, and so on. One problem arising in waveguide gratings is sidelobes which appear in their reflection spectrum [7], [8]. It was shown that by using apodization techniques for the longitudinal refractive index distribution of the waveguide grating, the sidelobes can be suppressed in the reflection spectrum of fiber Bragg gratings [8].

In this paper, apodized PC waveguide gratings are proposed to suppress sidelobes which appear in reflection spectra of usual PC waveguide gratings. By using specific functions (Gauss and Gauss-cosine functions) for the longitudinal refractive index distribution, it is possible to suppress sidelobes in the reflection spectra of PC waveguide gratings efficiently. The apodization is realized by simply changing diameters of dielectric pillars adjacent to the PC waveguide core. It is shown that by using Gauss-cosine functions for the apodization, the Bragg frequency of the waveguide grating becomes insensitive to the magnitude of perturbation thus leading to the possibility of designing waveguide gratings with arbitrarily Bragg frequency and bandwidth by modulating geometrical parameters only. All the simulations are done by using rigorous finite-element time-domain beam propagation method (FETD-BPM) [9], [10] to ensure accurate analysis. The parameters of the calculations are selected as follows $W = 10$, $R = 10^{-4}$, $\Delta T = 1$fs, and $N_{max} = 2\times10^{4}$, where W, R, ΔT, and N_{max} stand for the number of perfectly matched layers, the theoretical reflection coefficient, the time interval of calculations, and the number of the calculation steps, respectively.

2. Photonic crystal waveguide gratings with Gaussian apodization

Here, we consider a PC waveguide grating as shown in Fig. 1 composed of dielectric pillars (rods) on square array with lattice constant a, where the diameter of rods are taken as $d = 0.5a$. By assuming silicon-on-insulator configuration (SOI), refractive indexes of rods and background material are, respectively, taken as 3.4 (Si) and 1.45 (SiO_2). Experiments of the system of pillars have been already demonstrated in Refs. [11]-[13]. This PC has a PBG for TE modes which extends from $a/\lambda = 0.242$ to 0.289 with λ being the free-space wavelength. The propagating mode exists entirely in the PGB region. The waveguide core is formed by eliminating a row of rods, and the rods adjacent to both sides of the waveguide are alternately replaced by rods with different diameters to construct PC waveguide grating. The period is N and the diameters of modulated rods are d_n ($n = 1 \sim N$) as shown in Fig. 2. Usual PC waveguide gratings without apodization [7] are formed for $d_1 = d_2 = \cdots = d_n$. Here, Gaussian apodization is used for the longitudinal refractive index distribution of PC waveguide gratings. In this case, d_n is given by

$$d_n = d - d_c \exp\left[-\left\{ \frac{\left(n - \frac{N}{2}\right)\Lambda}{\omega_0} \right\}^2 \right] \tag{1}$$

where d_c is a maximum variation of the rod diameter, ω_0 is a spot size, and $\Lambda = 2a$ is a one period of grating. Figure 2 shows the longitudinal d_n variation of PC waveguide gratings with Gaussian apodization for $d_c = 0.05a$, $\omega_0 = 0.25N\Lambda$, and $N = 52$.

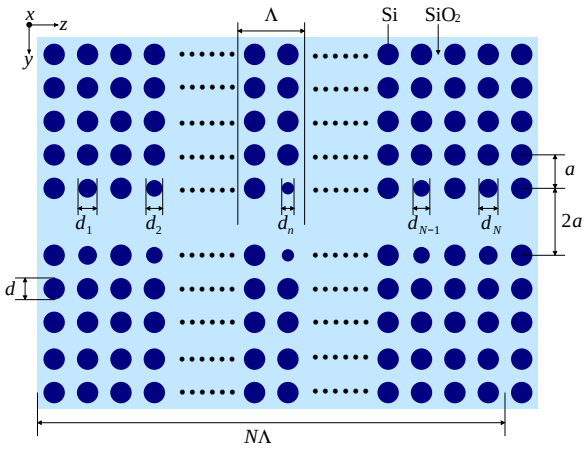

Fig. 1. PC waveguide gratings with Gaussian apodization composed of dielectric pillars on square array.

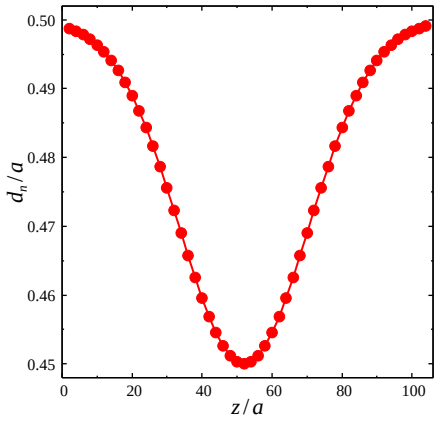

Fig. 2. Longitudinal d_n variation of PC waveguide gratings with Gaussian apodization for $d_c = 0.05a$, $\omega_0 = 0.25N\Lambda$, and $N = 52$.

Dashed line in Fig. 3 shows the reflection spectrum of the PC waveguide grating with Gaussian apodization for $d_c = 0.05a$, $\omega_0 = 0.25N\Lambda$, and $N = 52$, while the dash-dot line in Fig. 3 shows the reflection spectrum of the PC waveguide grating without apodization for $d_n = 0.45a$ and $N = 52$. We can see that the sidelobes in the reflection spectra are effectively suppressed by using apodization. However, reflection at the Bragg frequency is reduced. Solid line in Fig. 3 shows the reflection spectrum of PC waveguide gratings with Gaussian apodization for $d_c = 0.05a$, $\omega_0 = 0.25N\Lambda$, and $N = 104$. It is possible to obtain larger reflection for larger grating periods, however, small sidelobes appear in the lower frequency region.

Figure 4 shows the transmission spectra of PC waveguide gratings with Gaussian apodization ($d_c = 0.05a$ and $N = 104$) for different values of ω_0. Although larger reflections can be obtained by increasing the value of ω_0, sidelobes in lower frequency region also become larger. This is due to the fact that by increasing the value of ω_0, the longitudinal refractive index distribution comes closer to that of PC waveguide gratings without apodization.

Figure 5 shows the dispersion curves of the PC waveguide grating with $d_n = 0.45a$. We can see the anti-crossing of the propagating mode around the Bragg frequency.

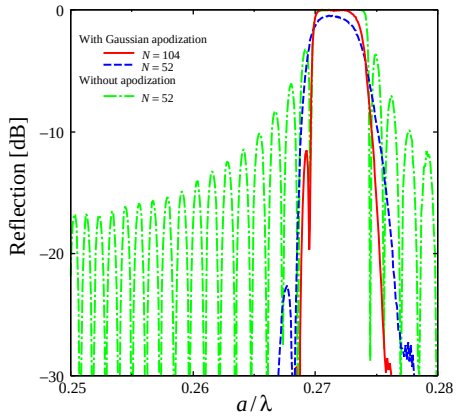

Fig. 3. Reflection spectra of the PC waveguide grating. Solid and dashed lines are reflection spectra of the PC waveguide grating with Gaussian apodization for $d_c = 0.05a$, $\omega_0 = 0.25N\Lambda$. The numbers of periods are 104 and 52, respectively. Dash-dot line shows reflection spectrum of PC waveguide gratings without apodization for $d_n = 0.45a$, $N = 52$.

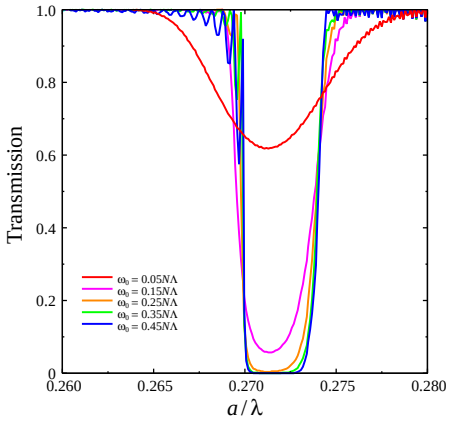

Fig. 4. Transmission spectra of the PC waveguide grating with Gaussian apodization ($d_c = 0.05a$ and $N = 104$), for different values of ω_0.

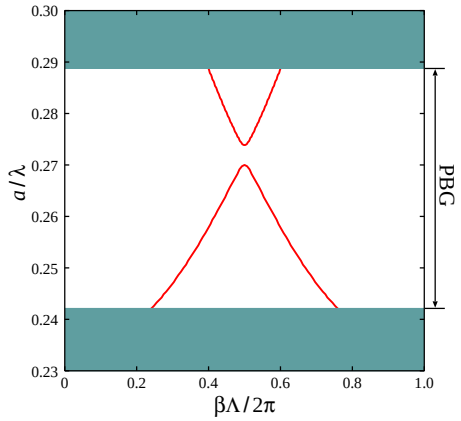

Fig. 5. Dispersion curves of the PC waveguide grating with $d_n = 0.45a$.

3. Photonic crystal waveguide gratings with Gauss-cosine apodization

Although the sidelobes in the reflection spectrum of PC waveguide gratings can be suppressed by using Gaussian apodization as shown in the previous section, the suppression is not enough in the low frequency region [8]. Here, PC waveguide grating with Gauss-cosine apodization is proposed to suppress sidelobes further. Figure 6 shows a PC waveguide grating with Gauss-cosine apodization. All the structural parameters with regard to PC are the same as in the previous section. To form Gauss-cosine PC waveguide gratings, diameters of rods adjacent to the core are changed to d_i ($i = 1 \sim 2N$) as shown in Fig. 6 which is given by

$$d_i = d + d_c \exp\left[-\left\{\frac{(i-N)\Lambda}{\omega_0}\right\}^2\right]\cos(i\pi). \tag{2}$$

Figure 7 shows one example of longitudinal d_i variation of PC waveguide gratings with Gauss-cosine apodization for $d_c = 0.025a$, $\omega_0 = 0.5N\Lambda$, and $N = 26$. In this case, rods with larger and smaller diameters are periodically arranged along with the envelope of the Gaussian function.

Solid, dashed, and dash-dot lines in Fig. 8 are reflection spectra of the PC waveguide grating with Gauss-cosine apodization ($d_c = 0.025a$, $\omega_0 = 0.5N\Lambda$, and $N = 104$), with Gaussian apodization ($d_c = 0.05a$, $\omega_0 = 0.25N\Lambda$, and $N = 104$), and without apodization ($d_{2j-1} = 0.5a$, $d_{2j} = 0.45a$, $j = 1, 2, \cdots, N$, and $N = 52$), respectively. The sidelobe appearing in the low frequency region in case of PC waveguide gratings with Gaussian apodization is well suppressed by utilizing Gauss-cosine apodization and the reflection spectrum is symmetric with respect to Bragg frequency.

Figure 9 shows transmission spectra of the PC waveguide grating with Gauss-cosine apodization ($d_c = 0.025a$ and $N = 104$) for different values of ω_0. Reflection at the Bragg frequency and sidelobes become larger for larger values of ω_0 as in the case of Gaussian apodization because of abrupt change of d_i. The tolerance of the spot size for the transmission coefficient at the Bragg frequency is shown in Fig. 10.

Though PC waveguide gratings can be constructed with the system of holes as well as that of pillars, the system of holes is particularly discussed in Ref. [7].

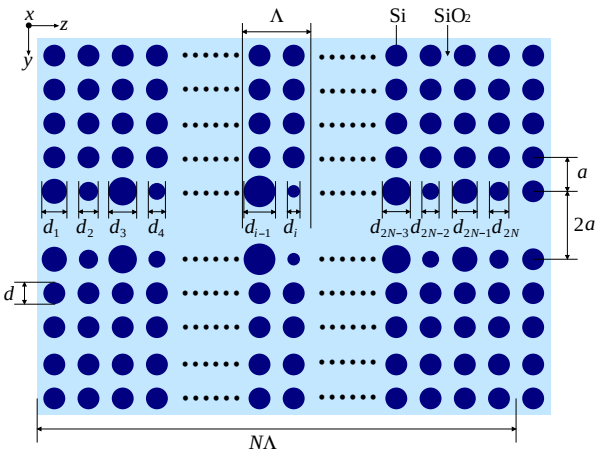

Fig. 6. PC waveguide gratings with Gauss-cosine apodization composed of dielectric pillars on square array.

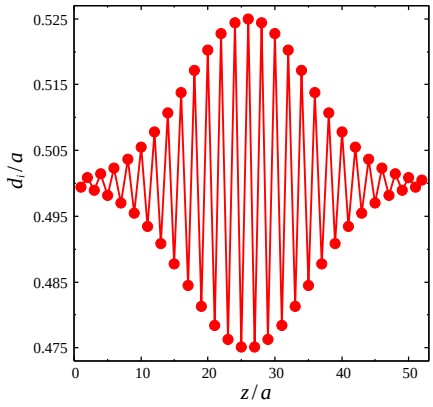

Fig. 7. Longitudinal d_i variation of PC waveguide gratings with Gauss-cosine apodization for $d_c = 0.025a$, $\omega_0 = 0.5N\Lambda$, and $N = 26$.

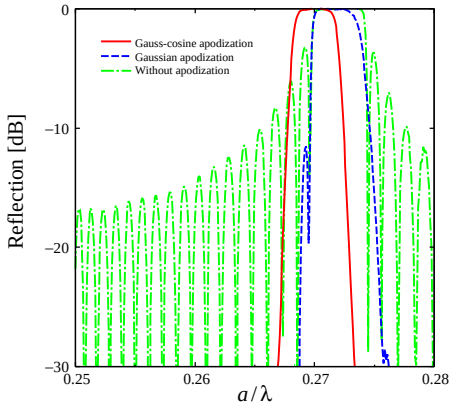

Fig. 8. Solid, dashed, and dash-dot lines are reflection spectra of PC waveguide gratings with Gauss-cosine apodization ($d_c = 0.025a$, $\omega_0 = 0.5N\Lambda$, and $N = 104$), with Gaussian apodization ($d_c = 0.05a$, $\omega_0 = 0.25N\Lambda$, and $N = 104$), and without apodization ($d_{2j-1} = 0.5a$, $d_{2j} = 0.45a$, $j = 1, 2, \cdots, N$, and $N = 52$), respectively.

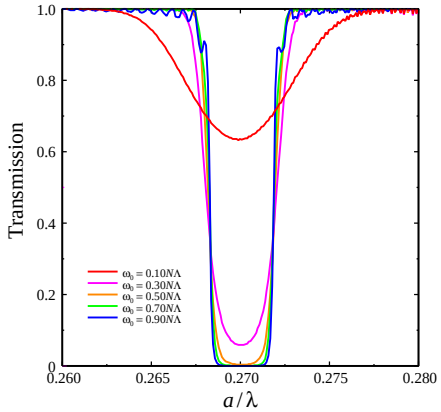

Fig. 9. Transmission spectra of PC waveguide gratings with Gauss-cosine apodization ($d_c = 0.025a$ and $N = 104$) for different values of ω_0.

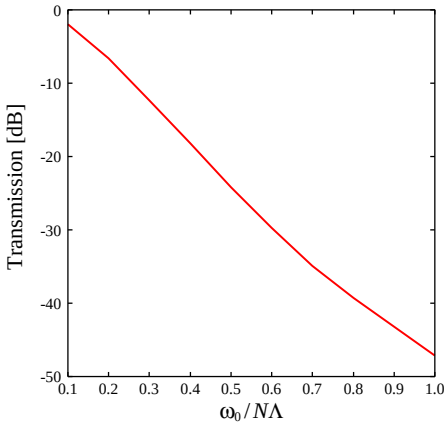

Fig. 10. The tolerance of the spot size for the transmission coefficient at the Bragg frequency.

4. Bragg frequency and bandwidth of photonic crystal waveguide gratings

The performance of waveguide gratings is characterized by their Bragg frequency, bandwidth, and reflection. These characteristics have to be carefully designed to meet the required performance. Reflection can be easily tuned by changing the number of periods of the grating. Bragg frequency and bandwidth can be tuned by changing the magnitude of refractive index in the grating. Because Bragg frequency and bandwidth of the grating are closely related to the magnitude of perturbation, both quantities are simultaneously changed for different perturbation. Therefore, it is difficult to make the Bragg frequency of the waveguide grating constant for different bandwidths. This is illustrated in Figs. 11 and 12. In particular, Figs. 11 and 12 show the transmission spectra of PC waveguide gratings for different values of d_c without apodization (N = 52) and with Gaussian apodization ($\omega_0 = 0.25N\Lambda$, and N = 104), respectively. For lager perturbation (larger values of d_c), larger bandwidth can be obtained and Bragg frequency is shitted to higher frequency region.

Figure 13 shows the transmission spectra of PC waveguide gratings with Gauss-cosine apodization for different values of d_c ($\omega_0 = 0.5N\Lambda$, and N = 104). Although larger bandwidth can be obtained for larger perturbation, Bragg frequencies are almost constant. This is quite unusual and can be explained as follows. Figure 14(a) shows one period of PC waveguide grating with Gauss-cosine apodization. This is composed of two PC waveguides, that is, a PC waveguide having rods with diameters d_{i-1} ($d_{i-1} > d$) adjacent to the core (we call it "waveguide A" hereafter) and a PC waveguide having rods with diameters d_i ($d_i < d$) adjacent to the core (we call it "waveguide B" hereafter). Solid, dashed, and dash-dot lines in Fig. 14(b) show dispersion curves of input PC waveguide, waveguide A with $d_{i-1} = 0.525a$, and waveguide B with $d_i = 0.475a$, respectively. Suppose β, β_A, and β_B are the propagation constants of input PC waveguide, waveguides A and B, and $\Delta\beta_A = \beta_A - \beta$ and $\Delta\beta_B = \beta - \beta_B$, Bragg condition is given by

$$\beta_A a + \beta_B a = \pi \tag{3}$$

or equivalently

$$2\beta a + (\Delta\beta_A - \Delta\beta_B)a = \pi. \tag{4}$$

According to Eq. (2), $|d - d_{i-1}| \approx |d - d_i|$, and therefore, $\Delta\beta_A \approx \Delta\beta_B$. In this case, Eq. (4) is reduced to $\beta a/2\pi = 0.25$. This means that Bragg frequency is constant regardless of the magnitude of perturbation and Bragg reflection occurs at the frequency satisfying above

condition. From Fig. 14(b), the frequency at which $\beta a/2\pi = 0.25$ is $a/\lambda = 0.27$ and this is consistent with the results of Fig. 13.

Figure 15 shows Bragg frequency $\omega_B = a/\lambda_B$ and bandwidth $\Delta\omega$ of PC waveguide gratings without apodization ($N = 52$, solid line), with Gaussian apodization ($\omega_0 = 0.25N\Lambda$, and $N = 104$, dashed line), and with Gauss-cosine apodization ($\omega_0 = 0.5N\Lambda$, and $N = 104$, dash-dot line) as a function of d_c. Here, λ_B is the wavelength at which the reflection is maximum and $\Delta\omega$ is defined as $|\omega_+ - \omega_-|$ where $\omega_\pm$ are frequencies at which transmission is 0.5. While Bragg frequency and bandwidth are simultaneously changed with d_c for PC waveguide gratings without apodization and with Gaussian apodization, Bragg frequency is almost constant for Gauss-cosine apodization. Usually, to obtain arbitrary Bragg frequency and bandwidth, both geometrical parameters and refractive indices of materials have to be modulated. By using Gauss-cosine apodization, PC waveguide gratings having arbitrary Bragg frequency and bandwidth can be simply designed by modulating the geometrical parameters only.

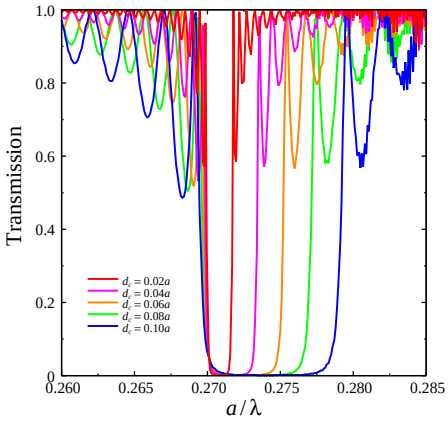

Fig. 11. Transmission spectra of the PC waveguide grating without apodization for different values of d_c ($N = 52$).

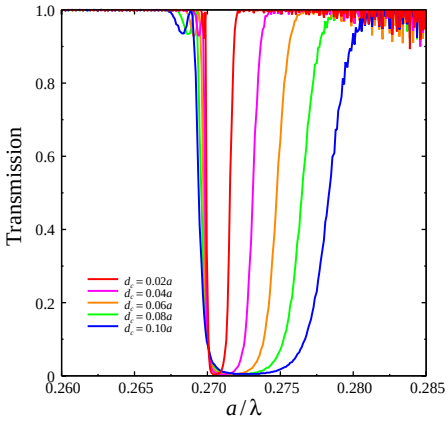

Fig. 12. Transmission spectra of the PC waveguide grating with Gaussian apodization for different values of d_c ($\omega_0 = 0.5N\Lambda$ and $N = 104$).

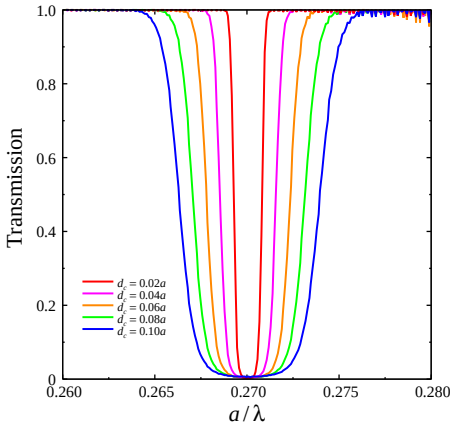

Fig. 13. Transmission spectra of the PC waveguide grating with Gauss-cosine apodization for different values of d_c ($\omega_0 = 0.25N\Lambda$ and $N = 104$).

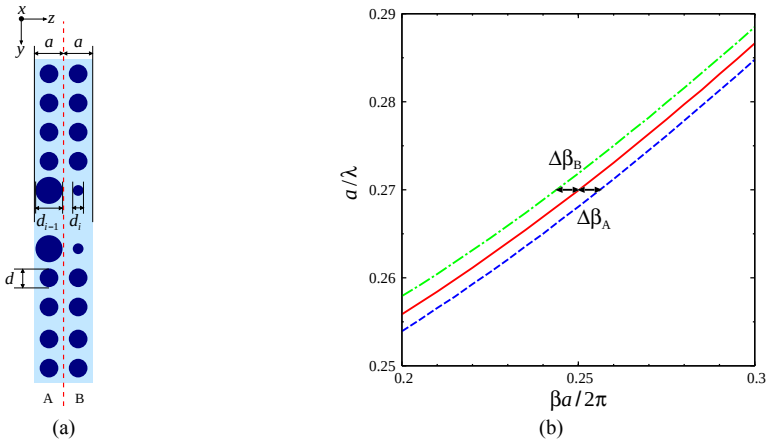

Fig. 14. (a) One period of the PC waveguide grating with Gauss-cosine apodization, and (b) the corresponding dispersion curves of the input PC waveguide (solid line), waveguide A with $d_{i-1} = 0.525a$ (dashed line), and waveguide B with $d_i = 0.475a$ (dash-dot line).

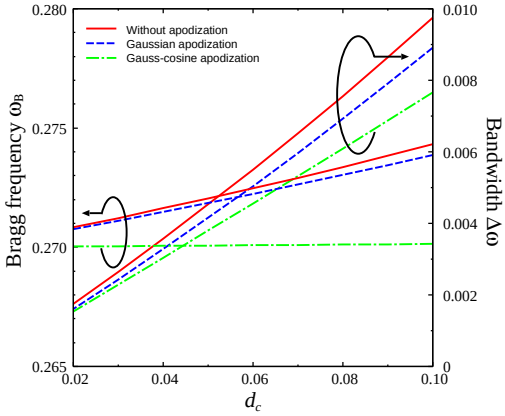

Fig. 15. Bragg frequency and bandwidth of PC waveguide gratings as a function of d_c.

5. Conclusions

We have proposed apodized PC waveguide gratings for suppressing the sidelobes appearing in the reflection spectra of usual PC waveguide gratings. It was shown that by using Gaussian and Gauss-cosine apodization, the sidelobes were effectively suppressed. The apodization can be realized by simply changing the geometrical parameters of PC waveguide gratings. Furthermore, it was shown that Bragg frequency of PC waveguide gratings with Gauss-cosine apodization is almost insensitive to the magnitude of perturbation leading to the possibility of designing PC waveguide gratings having arbitrarily Bragg frequency and bandwidth without modulating material properties. Although discussions about the application of PC waveguide gratings presented in this paper are limited to wavelength selective filter, other interesting applications of PC waveguide gratings may include slow light [14], because the group velocity of light can be slowed down near the stop band edge as in the coupled resonator optical waveguides [14].